J. Membrane Biol. 148, 65–78 (1995)

The Journal of
Membrane
Biology

A Method for Determining the Unitary Functional Capacity of Cloned Channels and Transporters Expressed in *Xenopus laevis* Oocytes

G.A. Zampighi[1], M. Kreman[1], K.J. Boorer[2], D.D.F. Loo[2], F. Bezanilla[2], G. Chandy[3], J.E. Hall[3], E.M. Wright[2]

[1]Department of Anatomy and Cell Biology, UCLA School of Medicine, Los Angeles, CA 90095-1763
[2]Department of Physiology, UCLA School of Medicine, Los Angeles, CA 90095-1751
[3]Department of Physiology and Biophysics, School of Medicine, University of California, Irvine, CA 92717

Received: 4 March 1995/Revised: 27 June 1995

Abstract. The *Xenopus laevis* oocyte is widely used to express exogenous channels and transporters and is well suited for functional measurements including currents, electrolyte and nonelectrolyte fluxes, water permeability and even enzymatic activity. It is difficult, however, to transform functional measurements recorded in whole oocytes into the capacity of a single channel or transporter because their number often cannot be estimated accurately. We describe here a method of estimating the number of exogenously expressed channels and transporters inserted in the plasma membrane of oocytes. The method is based on the facts that the P (protoplasmic) face in water-injected control oocytes exhibit an extremely low density of endogenous particles (212 ± 48 particles/μm^2, mean, SD) and that exogenously expressed channels and transporters increased the density of particles (up to 5,000/μm^2) only on the P face. The utility and generality of the method were demonstrated by estimating the "gating charge" per particle of the Na^+/glucose cotransporter (SGLT1) and a *nonconducting* mutant of the *Shaker* K^+ channel proteins, and the single molecule water permeability of CHIP (*Ch*annel-like *I*ntramembrane *P*rotein) and MIP (*M*ajor *I*ntrinsic *P*rotein). We estimated a "gating charge" of ~3.5 electronic charges for SGLT1 and ~9 for the mutant *Shaker* K^+ channel from the ratio of Q_{max} to density of particles measured *on the same oocytes.* The "gating charges" were 3-fold larger than the "effective valences" calculated by fitting a Boltzmann equation to the same charge transfer data suggesting that the charge movement in the channel and cotransporter occur in several steps. Single molecule water permeabilities (p_fs) of 1.4×10^{-14} cm^3/sec for CHIP and of 1.5×10^{-16} cm^3/sec for MIP were estimated from the ratio of the whole-oocyte water permeability (P_f) to the density of particles. Therefore, MIP is a water transporter in oocytes, albeit ~100-fold less effective than CHIP.

Key words: Freeze-fracture — Plasma membranes — Heterologous expression

Introduction

After the work of Barnard, Miledi & Sumikawa (1983), a large variety of channels, receptors and transporters and their genetically engineered and naturally occurring mutants have been expressed in *Xenopus laevis* oocytes and characterized by either electrophysiological or biochemical methods. Such studies have been highly effective in revealing overall functional differences between mutated versions of ion channels and transporters. However, the understanding of their mechanisms of action requires that functional measurements recorded in whole oocytes be normalized as the functional capacities of single channel, transporter or receptor. Often this transformation is hampered by difficulties in estimating the number of channels and transporters in the oocytes on which the functional measurements have been made. Methods used to estimate this number are either model-dependent or require specific, high-affinity ligands which are unavailable for many channels and transporters.

This paper describes a method that estimates the number of exogenously expressed cloned channels and transporters from the density of intramembrane particles inserted in the plasma membrane (oolemma) of *Xenopus* oocytes. The method is based on the facts that water-injected control oocytes exhibit a surprisingly low den-

Correspondence to: G.A. Zampighi

sity of endogenous proteins inserted in the oolemma and that exogenous channels and transporters appear on the P (protoplasmic) fracture face. An important feature of the method is that both the density of intramembrane particles and functional properties of channels and transporters, such as charge transfer, water permeability or conductance, can be measured *on the same oocyte.*

The effectiveness and generality of the method was demonstrated by estimating the "gating charge" per particle of the Na^+/glucose cotransporter (SGLT1) and of a nonconducting mutant of the *Shaker* K^+ channel, and the single-molecule water permeability of CHIP (*Ch*annel-like *I*ntramembrane *P*rotein) and MIP (*M*ajor *I*ntrinsic *P*rotein). For SGLT1 and the mutant *Shaker* K^+ channel, the "gating charge" was estimated from the ratio of the maximum number of charges translocated across the oolemma in response to voltage pulses (Q_{max}) to the density of intramembrane particles. The value of the gating charge estimated with this method was ~3-fold larger than that calculated by fitting a Boltzmann equation to the same charge transfer data. Thus, the number of channels and transporters estimated from the density of intramembrane particle provides independent cross checks and constraints on models of channel function based on analysis of charge transfer data.

For MIP, CHIP and SGLT1, the density of particles and the water permeability (P_f) were measured in oocytes from the same batch. Comparison of the estimated values of the water permeability per molecule (p_f) of a *bona fide* water channel (CHIP) and SGLT1 indicated that MIP is a water transporter, albeit 100-fold less effective than CHIP. Thus, freeze-fracture electron microscopy provides accurate estimates of the number of exogenous channels and transporters inserted in the oolemma. From the ratio of functional properties and the density of particles, both measured on the same oocyte, a variety of single-molecule capacities of channels and transporters can be estimated.

Materials and Methods

Oocyte Preparation

Stage VI *X. laevis* oocytes were removed from female frogs and processed in one of two ways. At UCLA, they were defolliculated by treatment with collagenase B as described previously (Parent et al., 1992). At UCI, they were defolliculated by treating them twice, for 90 min, with 2 mg/ml collagenase B. The oocytes were washed with Ca^{2+}-free saline solution (in mM: 82.5 NaCl, 2.5 KCl, 1 $MgCl_2$, 5 HEPES) and allowed to recover overnight in ND96 medium (in mM: 96 NaCl, 2 KCl, 1.8 $CaCl_2$, 1 Mg Cl_2 and 5 HEPES, pH 7.4) plus supplements (2.5 mM sodium pyruvate, 10 μg/ml aminobenzylpenicillin and 10 μg/ml streptomycin) at 18°C.

Control oocytes were injected with 50 nl of distilled water. Oocytes expressing SGLT1 and the mutant *Shaker* K^+ channels were injected with 50 nl of a solution containing 1 μg/μl of either rabbit SGLT1 cRNA (Parent et al., 1992) or cRNA coding for the W434F mutant of the H4-1R *Shaker* B K^+ channel (Perozo et al., 1993). Oocytes expressing MIP and CHIP were injected with 50 nl of a solution of cRNA coding for bovine MIP and human CHIP flanked by *Xenopus* β-globin 5′ and 3′ untranslated regions (Gorin et al., 1984; Preston & Agre, 1991; Preston et al., 1992; Mulders et al., 1995). RNAs were produced from Bluescript plasmids (provided to us by Dr. P. Agre). CHIP and MIP plasmids were linearized with Xba I and the capped RNA synthesized with T3 RNA polymerase. The cRNAs were precipitated in ethanol, resuspended in DEPC treated water and stored at −70°C. All injections were performed using positive-displacement micropipettes.

Electron Microscopy

Fixation

After the appropriate functional property was measured, oocytes were fixed sandwiched between two glass slides separated by 200 μm thick spacers (Fig. 2, panels *a* and *b*). This procedure flattened oocytes into oblates, a geometry that greatly simplified obtaining large areas of fracture faces of the oolemma. The fixative solution was 3–3.5% glutaraldehyde in 0.2 M Na cacodylate pH 7.4. After 15 min, the oocytes were removed from the slides and immersed in the same fixative solution for 1 hr, at room temperature (Fig. 2, panel *d*).

Thin Sectioning

The flattened oocytes were postfixed in 1% OsO_4 in 0.2 M Na cacodylate buffer for 90 min at room temperature. They were washed in 0.1 M Na acetate buffer pH 5.0 and block stained in 0.5% uranyl acetate in 0.1 M Na acetate buffer pH 5.0 overnight at 4°C. The oocytes were dehydrated in ethanol, passed through propylene oxide and embedded in Epon 812. Sections were cut in a Sorval MT5000 ultramicrotome, collected on single-hole, formvar-coated grids and stained on the grids with uranyl acetate and lead (Zampighi et al., 1988).

Freeze Fracture

The oblate-shaped oocytes were infiltrated with 25% glycerol in 0.2 M Na cacodylate pH 7.4 for 1 hr at room temperature. They were cut first in halves and then into 4–6 smaller pieces which were placed on Balzers specimen holders with the external surfaces (i.e., the vitelline membrane) facing upward. This precaution greatly increased the chances of fracturing P instead of E faces (Fig. 2, panel *e*). The specimens were frozen by immersion in liquid propane cooled in a liquid nitrogen bath. The frozen oocytes were transferred into a Balzers 400K freeze-fracture-etch apparatus, fractured at either −150°C or −120°C and at 1×10^{-7} mbar of partial pressure. The fractured surfaces were coated with platinum at 80° and carbon at 90°. Shadowing at 80°, instead of 45° produced intramembrane particles with shorter shadows which facilitated their quantification, particularly in replicas from oocytes that exhibited the highest densities (~5,000/μm^2). The replicated specimens were coated with 0.5% collodion in amyl acetate (to avoid fragmentation of the replica) and cleaned in a solution of bleach. The replicas were washed in distilled water and deposited on formvar-coated copper grids. The collodion was removed by immersion in amyl acetate (Zampighi et al., 1988).

Sampling

The large total area of the oolemma ($3–6 \times 10^7$ μm^2) introduces sampling problems because freeze-fracture and morphometric methods can

Table 1. Gating charges of SGLT1 and *Shaker* K

Oocyte	Charge transfer (nC)	Capacitance (nF)	Particle density[a] (μm^2)	Charge density (μm^2)	Gating charge
[c]SGLT1	4	335	210 ± 55 (8)	746	3.6
[c]SGLT1	11.5	366	556 ± 108 (12)	1,967	3.6
[c]SGLT1	16	488[d]	655 ± 67 (8)	2,049	3.1
[b]K^+-Channel	1.66	28.4	368 ± 105 (19)	3,259	8.9
[b]K^+-Channel	3.2	31.8	698 ± 110 (5)	6,289	9.0

[a] The particle density was determined from 3–4 replicas from the *same* oocytes. To all particle densities listed in this column, the density of particles measured in water-injected oocytes (212 ± 48 particles/μm^2, n = 14) has been subtracted. The numbers in parenthesis correspond to the number of P fracture faces used to calculate the mean and SD.

[b] The measurements were obtained using the cut-open oocyte technique (Stefani et al., 1994) that used a hole of about 600 μm diameter.

[c] The measurements were obtained using the 2-electrodes voltage clamp technique in whole-oocyte (Loo et al 1993).

[d] The capacitance of oocytes expressing SGLT1 increases with expression (J.R. Hirsch, D.D.F. Loo and E.M. Wright, *unpublished observations*).

process only a small percentage of the total area of the oolemma (10^2 or 10^3 μm^2). Collection of 4–6 replicas from the same oocyte guarantee that the particle density of different regions will be included in the quantification. The replicas were inspected in the electron microscope and fracture faces from the oolemma imaged at 25,000×. The negatives (100–300 per replica) were inspected under a stereomicroscope to determine whether the particles distributed randomly or in patches in the fracture faces of the oolemma, the folds and the microvilli. From this pool of negatives, 4–6 negatives per replica were selected for quantification. The selection criterion required that the images were free of optical aberrations, contain 3–5 μm^2 of *uninterrupted* P fracture face and were representative of the pool from which they were selected.

This sampling procedure was validated by measuring charge transfer (Q_{max}) and particle density in a series of oocytes expressing different amounts of either *Shaker* K^+ channels or SGLT1. We reasoned that if oocytes exhibiting different amounts of proteins maintained a constant ratio of Q_{max} to particle density, this would be a strong indication that the density of intramembrane particles represents the number of channels and transporters in the oolemma (Table 1).

Quantification

Images of the P fracture faces were enlarged at 75,000× final magnification and digitized in a Microtex ScanMaker 600 Zs at 200 dpi. The digitized images were analyzed on a Macintosh IIfx computer using IMAGE 1.54 software package (written by W. Rasband at the U.S. National Institutes of Health and available from the Internet by anonymous ftp from zippy.nimh.nih.gov or on floppy disk from NTIS, 5285 Port Royal Rd. Springfield, VA 22161, part number PB93-504868.). In each micrograph, we measured the area of the P fracture face and counted the number of intramembrane particles present. Although fracture faces from microvilli were not included in the quantification (because their strong curvatures interfered with shadowing), inspection and quantification showed that the particle distribution was not significantly different from that of the oolemma (*see* Fig. 5).

Area Measurements

If oocytes were smooth spheres 1 mm in diameter, they would have an area of ~3×10^6 μm^2. However, the presence of folds and microvilli greatly increase the surface area of the oolemma. The area of folds were estimated from freeze-fracture replicas. We noticed that the fracture faces of the oolemma contained "interruptions" that arose when the fracture plane passed from the oolemma into the cytoplasm (Figs. 9*A* and 10*A*). They were interpreted to be fractures through the folds. In 52 μm^2 of P face, the "interruptions" occupied ~10 μm^2 or ~20% of the area. Folds were modeled as five-side cubes to calculate their area (5×0.2 μm^2) and, by this model, they double the surface area of the oolemma.

The area of membrane in microvilli was estimated to be equal to 20–23 $\times$ 10^6 μm^2 by multiplying the area of each microvilli times the number of microvilli in the oocyte. Each microvilli measured 1.4 ± 0.9 μm (mean, SD, n = 7) in length and 0.12 ± 0.03 μm in diameter (mean, SD, n = 26). A cylinder with these dimensions has an area of 0.53 μm^2. The number of microvilli per oocyte was estimated to be 38–44 $\times$ 10^6 by multiplying the area of the oocyte (6.3×10^6 μm^2) by the density of microvilli (6–7 microvilli per μm^2) estimated from freeze-fracture replicas (Fig. 3*B*). Thus, the total area of the plasma membrane of a water-injected oocyte is 8.5–9.5-fold the area of a smooth sphere of the same diameter. Similar estimates for the area of the plasma membrane were obtained for *Buffo* oocytes (Dick & Dick, 1970).

Resolution of the Method

It was also important to determine the upper and lower limits of particle densities which can be quantified on the P face of the oolemma. The lower limit was conservatively taken as 100 particles/μm^2 above the mean density measured in control oocyte. This is two standard deviations above the average particle density of water-injected oocytes (confidence level of 98%). The upper limit was 5,000 particles/μm^2 and corresponds to the highest density of particles that was quantified accurately.

Others

The diameter of the intramembrane particles was measured directly from the negatives using a Nikon Comparator. The study summarizes results of 14 replicas from water-injected oocytes, 22 replicas from oocytes expressing SGLT1, 11 replicas from oocytes expressing the mutant *Shaker* K^+ channels, 6 replicas from oocytes expressing MIP and 4 replicas from oocytes expressing CHIP. Over 3,500 negatives were collected from these replicas of the P face of the oolemma.

Q_{max} Measurements

SGLT1

Oocytes, incubated in (mM): 100 NaCl, 2 KCl, 1 $CaCl_2$, 1 $MgCl_2$ and 10 HEPES/Tris pH 7.4, were voltage clamped using a 2-electrode

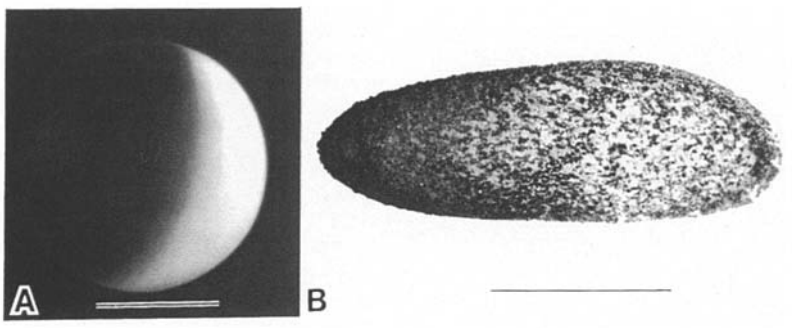

Fig. 1. Panel *A* shows a defoliculated *X. laevis* oocyte that was maintained in culture medium for 3 days. The animal (black) and vegetative (light) poles are clearly visible. An oocyte of this diameter possess a total plasma membrane area of 2.6–2.9 × 10^7 μm^2, most of which (2–2.3 × 10^7 μm^2) is located in the microvilli. Magnification: ×40, Bar 250 μm. Panel *B* shows a thick section of a plastic-embedded oocyte prepared with the "squeeze-fix" method described in Fig. 2. The oocyte appears as an ellipse with short and long axes measuring about 600 μm and 200 μm, respectively. Magnification: ×125, calibration bar: 250 μm.

voltage clamp method as described previously (Loo et al., 1993). The membrane potential of the oocyte was held at −50 mV and the currents were measured after the membrane potential was stepped for 100 msec to various potentials ranging from −150 to +50 mV. The total current $I(t)$ was fitted to $I(t) = I_1\exp(-t/\tau_1) + I_2\exp(-t/\tau_2) + I_{ss}$, where t is the time after onset of the voltage step, I_1 is the oocyte membrane capacitive current with time constant τ_1, I_2 is the SGLT1 transient current with time constant τ_2 and I_{ss} is the steady-state current. The transient currents due to SGLT1 were obtained by subtracting the capacitive current ($I_1\exp(-t/\tau_1)$ and steady state current (I_{ss}) from the total current, $I(t)$. The transient currents recorded at each test voltage were integrated to obtain the amount of charge transferred (Q). Plots of Q against V (Fig. 6*B*) exhibited a sigmoidal relationship well fit by the Boltzmann equation: $Q = Q_{max}/[1 + \exp\{(V\text{-}V_{0.5})zF/RT\}]$, where Q_{max} ($Q_{dep} - Q_{hyp}$) is the maximal charge transfer, Q_{dep} and Q_{hyp} are the charge movements at the depolarizing and hyperpolarizing limits, $V_{0.5}$ is the potential for 50% Q_{max}, z is the apparent valence of the movable charge, F the Faraday constant, R the gas constant, and T the absolute temperature. The curve in Fig. 6*B* was drawn with Q_{max} = 62 nC, $V_{0.5}$ = +9 mV and an "effective valence", z = 1.0. The number of SGLT1 molecules, N, in the oolemma was calculated from the formula $N = Q_{max}/ze$, where e is the elementary charge. This value of N will be compared with the model-independent value estimated from the density particles on the P (protoplasmic) fracture face of the oolemma.

K^+ Channels

Oocytes expressing the mutant *Shaker* K^+ channels were studied electrophysiologically using the cut-open oocyte technique (Tagliatela et al., 1992) as modified by Stefani et al., 1994. Charge transfer was estimated by integrating the transient currents recorded after pulsing the membrane from the holding potential of −90 mV to test potentials between −90 and +20 mV. Channel gating currents were corrected for capacitative currents obtained by the P/4 method (Bezanilla & Armstrong, 1977). The membrane capacitance was estimated from the integral of the current resulting from a pulse from −90 to −100 mV, where the gating currents are negligible. The Q/V curve (Fig. 6*C*) was approximated by a single Boltzmann relation with a Q_{max} of 1.38 nC, $V_{0.5}$ of −46 mV and an effective valence of 3.3. As discussed by Bezanilla et al., 1994, the data were better fit with two Boltzmann relations: $Q^1_{max} = 0.57$ nC, $Q^2_{max} = 0.79$ nC, $z^1 = 3.3$, $z^2 = 4.5$, $V^1_{0.5} = -.54$ mV and $V^2_{0.5} = -41$ mV.

Water Permeability Measurements

Water permeability was calculated from changes in the cross sectional area of oocyte challenged with media diluted 70%, at 10°C (Zhang & Verkman, 1991). The cross-sectional area was measured as a function of time from bright field images collected every 5 sec. The images were digitized with a frame grabber (LG3 Scion, Maryland) connected to a CCD camera (wv-BD400 Panasonic) and the cross-sectional areas were calculated with an algorithm in the public domain program NIH Image 1.54 running in a Macintosh (Power PC 8100). The temperature of the medium was maintained at 10°C with a Peltier device (Model 5000 KT stage controller, 20/20 Technology) and monitored continuously with a micro thermistor (TH-1 Thermistor Probe) placed close to the oocyte in the bath.

The cross-sectional area (A) was used to calculate the relative volume of oocytes (V/V_o) from the equation: $(A/A_o)^{3/2} = V/V_o$, where A_o is the cross-sectional area at time = 0, V is the volume as a function of time and V_o is the volume at time = 0. Osmotic water permeability was calculated from the formula: $P_f = \{d(V/V_o)/dt\}\{V_o/S_o\}/\{\Delta_{osm}v_w(S_{real}/S_{sphere})\}$, where S_o is the geometric surface area of the oocyte at time zero, Δ_{osm} is the osmotic gradient measured with a vapor pressure osmometer (A Wescor-5500), v_w is the partial molar volume of water, S_{real} is the area of the oolemma after correcting for the presence of folds and microvilli and S_{sphere} is the area calculated by assuming a sphere. Morphological estimates indicated that S_{real}/S_{sphere} was equal to 9 (*see below*).

Results

Water-injected, Control Oocytes

Area Measurements

Defolliculated oocytes appear as large, smooth spheres having dark (animal) and light (vegetative) poles (Fig. 1*A*). Oocytes are not, however, smooth spheres but their surface contains folds (black arrows Fig. 3*A*) and microvilli (empty arrows Fig. 3*A*) that greatly increase the surface area of the oolemma. We estimated that folds double the area of the oolemma and that microvilli increase the area by 20–23 × 10^6 μm^2. Therefore, a 1 mm diameter, water-injected oocyte has a plasma membrane

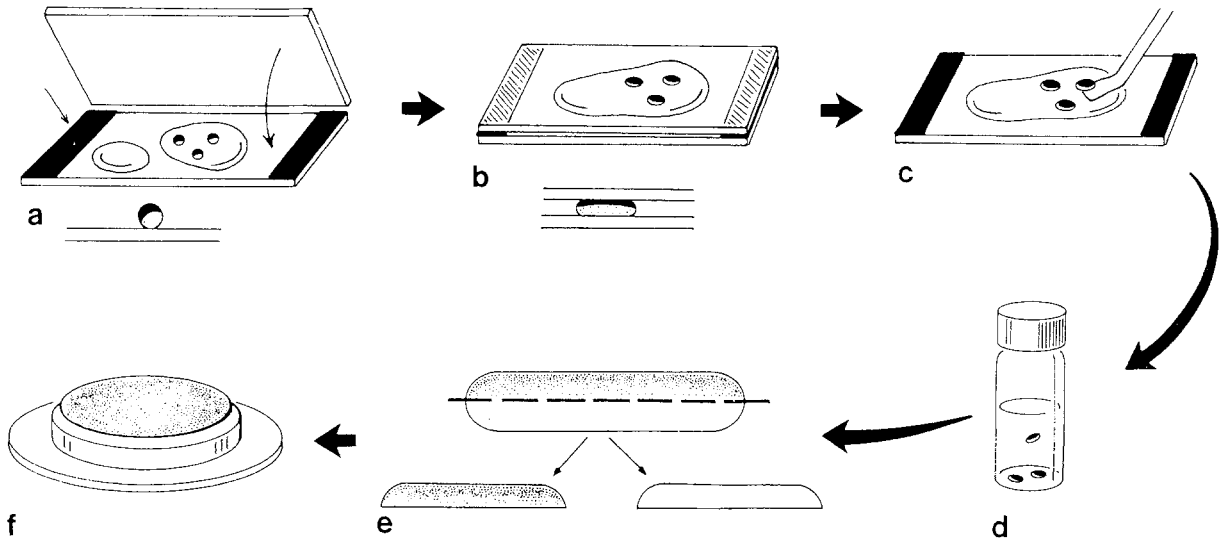

Fig. 2. Diagram summarizing the steps used to prepare oocytes for electron microscopy. After water permeability or charge transfer and total membrane capacitance were measured, oocytes were placed on glass cover slides with stainless steel spacers 200 μm in thickness (dotted arrows panel *a*). Fixative solution was deposited on top of the oocytes and the cells were squeezed immediately with another glass cover slide (panel *b*). This simple procedure transforms the spherical oocytes into oblates, a geometry which facilitated the fracture of large areas of oolemma. The oocytes were fixed between the glass slides for about 15–30 min after which they were removed from the glass with a spatula (panel *c*) and fixed for 1 hr at room temperature (panel *d*). The oocytes were washed in 0.2 M Na cacodylate buffer, infiltrated with 25% glycerol and cut into 4–6 smaller pieces (panel *e*). The pieces were placed on Balzers specimen holders (panel *f*) with the external surface (i.e., the vitelline membrane) facing upward to improve the chances in obtaining P instead of E faces. Exogenously expressed SGLT1, K^+ channels, CHIP and MIP molecules increased the density of particles on the P face only.

area of 26–29 × 10^6 μm^2, which is 8.5–9.5-fold greater than the area calculated by modeling the oocyte as a smooth sphere (~3 × 10^6 μm^2).

The area of the oolemma of water-injected oocytes was also estimated from measurements of the total capacitance. Control oocytes exhibited capacitance that extended over a range of 275 nF to 340 nF from where plasma membrane areas of 27.5 to 34 × 10^6 μm^2 were calculated assuming a specific capacitance of 1 $\mu F/cm^2$. Therefore, both morphological and electrophysiological measurements indicate that the area of the oolemma of oocytes is ~10-fold larger than the area calculated by assuming that they are smooth spheres.

Freeze Fracture

Our first attempts at estimating the density of intramembrane particles in the oolemma were unsuccessful because of the difficulty in sampling large areas of fracture faces of the oolemma from a given oocyte. Oocytes are large spheres and, most often, the fracture plane passed into the cytoplasm instead of following the fracture plane offered by the oolemma. This produced replicas containing exceedingly small and fragmented (discontinuous) areas of fracture faces of the oolemma. We solved this technical problem by sandwiching oocytes between two glass microscope slides during fixation (Fig. 2). The flattened oocytes (Fig. 1*B*) produced replicas containing *large areas of continuous fracture faces of oolemma* required for the quantification of intramembrane particle density.

The extensive fracture faces obtained with the squeeze-fix method allowed the unequivocal identification of both P (protoplasmic) and E (external) fracture faces of the oolemma and the quantification of their density of endogenous intramembrane particles. The P and E fracture faces of the oolemma were identified from the fracture pattern of microvilli. These surface specialization appeared as highly elongated convex and concave fracture surfaces (Figs. 3*B* & 4). The convex surface corresponds to the P (protoplasmic) face and the concave surface to the E (external) face of the oolemma. In control water-injected oocytes, the E face contained large diameter (14 ± 1.2 nm; n = 30) particles at a density of 886 ± 36 particles/μm^2 (mean, SD, n = 7, mean area counted = 0.52 μm^2) (Figs. 4 & 5). The P face, on the other hand, contained smaller diameter (7.2 ± 0.5 nm; n = 40) particles at a density of 212 ± 48 particles/μm^2 (mean, SD, n = 19, mean area counted = 0.75 μm^2) (Figs. 4 & 5). Since the channels and transporters studied here appeared as particles on the P face only, the low density of endogenous particles in this fracture face allowed their quantification with great accuracy and high confidence (*see* below).

Bluemink et al. (1983) reported that defolliculated oocytes exhibited endogenous intramembrane particles

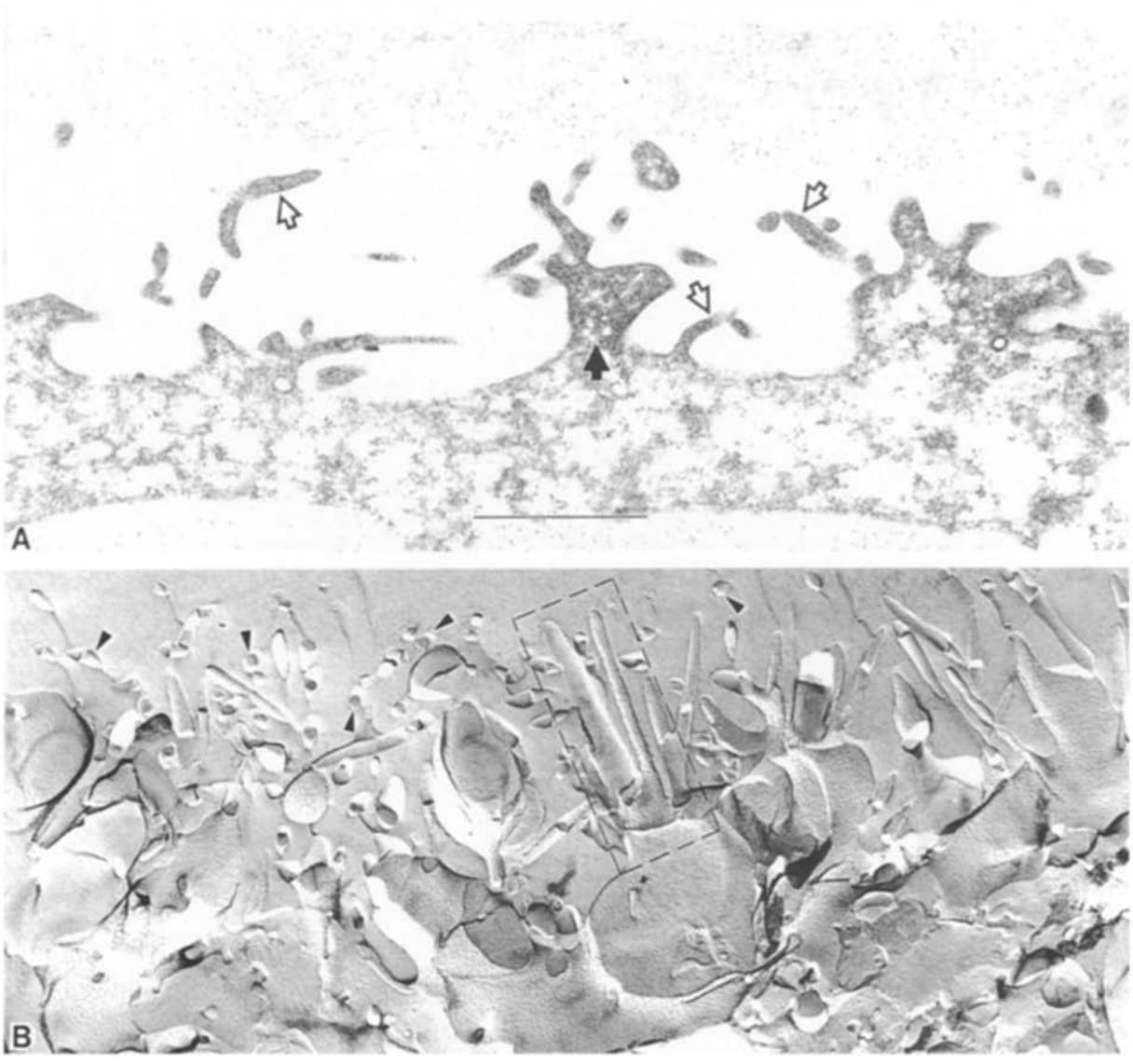

Fig. 3. Water-injected, control oocytes. Panel *A* shows a thin section electron micrograph of the surface of a squeeze-fixed oocyte. Folds and microvilli are located in a space about 1 μm wide located between the vitelline membrane and the oocyte' surface. Folds appear as irregularly-shaped elevations of the oocyte' surface (solid black arrow). Microvilli appear as long, cylindrical projections originating from folds and the oolemma (empty arrows). Panel *B* is a freeze-fracture replica of a squeeze-fixed oocyte. The replica shows fracture faces arising from the oolemma, folds and the microvilli. Microvilli were fractured either perpendicular (arrowheads) or along their long axis (area inside rectangle). Magnification *A* and *B:* ×25,000, calibration bar: 250 μm.

on the P face at a density that is four times lower than the density estimated in our controls (50 particles/μm^2 vs. 212 particles/μm^2). Such a difference probably arises from differences in the treatment of the oocytes. Our controls were injected with water and incubated for three or more days in media whereas those oocytes quantified by the Bluemink et al. (1983) were uninjected and maintained for a few hours in media.

SGLT1 and the Mutant *Shaker* K^+ Channel

Injection of cRNA coding for the Na^+/glucose cotransporter (SGLT1) and a mutant *Shaker* K^+ channel increased the density of particles only on the P face of the oolemma (Figs. 7–9). This result was fortunate because this fracture face exhibits an extremely low particle density in water-injected, control oocytes. For a given batch of cRNA-injected oocytes, the particle density always increased with the time of incubation, indicating that the new particles were, at the very least, induced by the injection. Oocytes injected with cRNA coding for SGLT1 increased their particle density very rapidly. In one experiment, we estimated 768 ± 156 particles/μm^2 (mean ± SD, n = 24, mean area counted = 0.32 μm^2) on day one and 4,521 ± 950 particles/μm^2 (mean ± SD, n =

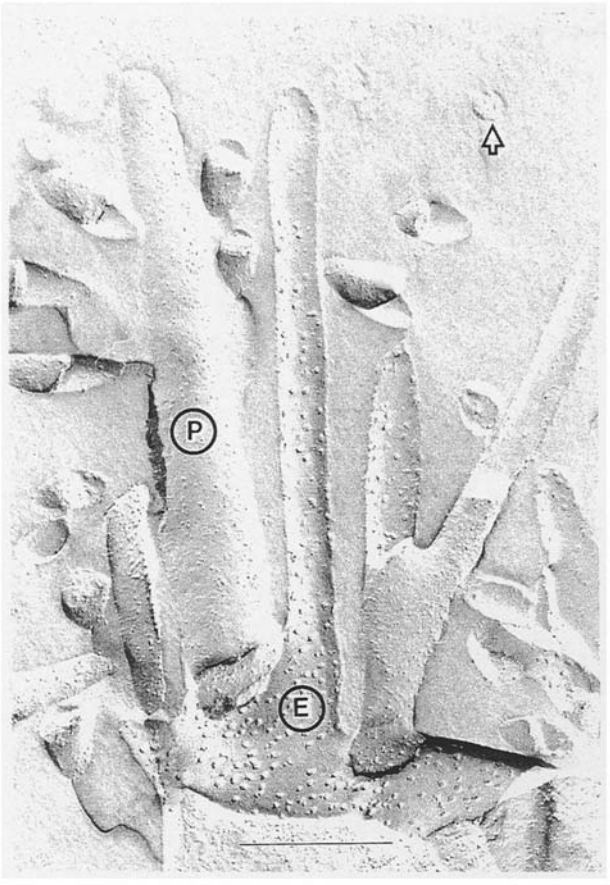

Fig. 4. Higher magnification of the area inside the rectangle in Fig. 3*B*. Microvilli that fractured along their long axis appear as concave (E face) and convex (P face) surfaces. The concave E fracture face is characterized by the presence of ~14 nm diameter intramembrane particles. The convex P fracture face was characterized by ~7 nm diameter particles. The arrow points to a microvilli in cross-section. Magnification: ×100,000, calibration bar: 0.3 μm.

11, mean area counted = 0.19 μm^2) on day two. Thus, as more of the exogenous protein is expressed, more particles appear on the P face of the oolemma.

To show that the new particles seen on the P faces corresponded to SGLT1 and the mutant *Shaker* K^+ channels, we measured the particle density and the charge transfer, Q_{max} on the *same oocytes*. Q_{max} is the maximum nonlinear charge translocated across the membrane in response to a voltage pulse. Therefore, the particles will correspond to either SGLT1 (Fig. 8) or the mutant *Shaker* K^+ channels (Fig. 9) only if the ratio of Q_{max} to particle density remains constant at different levels of expression.

We analyzed the particle density of oocytes expressing SGLT1 that measured Q_{max} of 4 nC (210 ± 55 particles/μm^2, mean ± SD, n = 8, mean area counted = 0.95 μm^2), 11.5 nC (556 ± 108 particles/μm^2, mean ± SD, n = 12, mean area counted = 0.45 μm^2) and 16 nC (655 ± 67 particles/μm^2, mean ± SD, n = 8, mean area counted = 0.6 μm^2). From the measurement of Q_{max} and capacitance, we estimated the density of charge per unit area. From the ratio of charge density to particle density ($7.5 \times 10^2/210$; $2.0 \times 10^3/556$ and $2.0 \times 10^3/655$), we estimated a value 3.1–3.6 electronic charges per particle (Table 1). For the mutant *Shaker* K^+ channels, Q_{max} and capacitance were measured in the cut-open oocyte preparation instead of the whole oocyte preparation used for SGLT1. In oocytes measuring Q_{max} of 1.66 nC (368 ± 105 particles/μm^2, mean ± SD, n = 19, mean area counted = 0.98 μm^2) and 3.2 nC (698 ± 110 particles/μm^2, mean ± SD, n = 7, mean area counted = 0.98 μm^2), we estimated ~9 electronic charges per particle ($3.3 \times 10^3/368$ and $6.3 \times 10/698$). In an oocyte with a Q_{max} of only 0.2 nC, we measured only 30 particles/μm^2 above background and the ratio of Q_{max} to the particle density estimated a gating charge per particle of ~10 electronic charges. This oocyte was not listed in Table 1, however, because the mean particle density in the patch was less than 2 SD greater than the mean particle density in control oocytes (212 ± 48 particles/μm^2).

A conclusion of the studies correlating the particle density to the density of charges was that the ratio of Q_{max} to particle density was independent of the level of protein expression, a fact that indicates that the particles must be either SGLT1 or mutant *Shaker* K^+ channels.

The intramembrane particles corresponding to mutant *Shaker* K^+ channels measured 10.7 ± 0.9 (mean, SD, n = 44) nm in diameter. Those corresponding to SGLT1, on the other hand, measured 7.5 ± 0.6 (n = 41) nm in diameter. Both proteins exhibit similar polypeptide molecular weight (about 70 kD), thus, the difference in particle size could reflect differences in their structure (i.e., the number of transmembrane domains) or the number of monomers composing the functional unit. Since *Shaker* K^+ channels are tetramers (MacKinnon, 1991; Li et al., 1994), each 7.5 nm diameter SGLT1 particle is probably a monomer or a dimer.

Quantification of particle density as function of the time of incubation after cRNA injection provided estimates of the net rate of synthesis and insertion of SGLT1. In one batch of oocytes expressing SGLT1, we measured ~5,000 particles/μm^2 (or $\sim 1.5 \times 10^{11}$ particles per oocyte) about 50 hr post injection. Therefore, SGLT1 was inserted into the oolemma at a rate of ~1 million particles per second per oocyte or 1 particle per μm^2 every ten seconds ($1.5 \times 10^{11}/1.8 \times 10^5$). This estimate emphasizes the efficiency of the machinery involved in the synthesis and insertion of channels and cotransporter in the oolemma.

Taken together, the results gathered from oocytes expressing SGLT1 and the mutant *Shaker* K^+ channel proteins demonstrate that freeze-fracture methods provide accurate estimates of the total number of channels and transporters inserted in the oolemma.

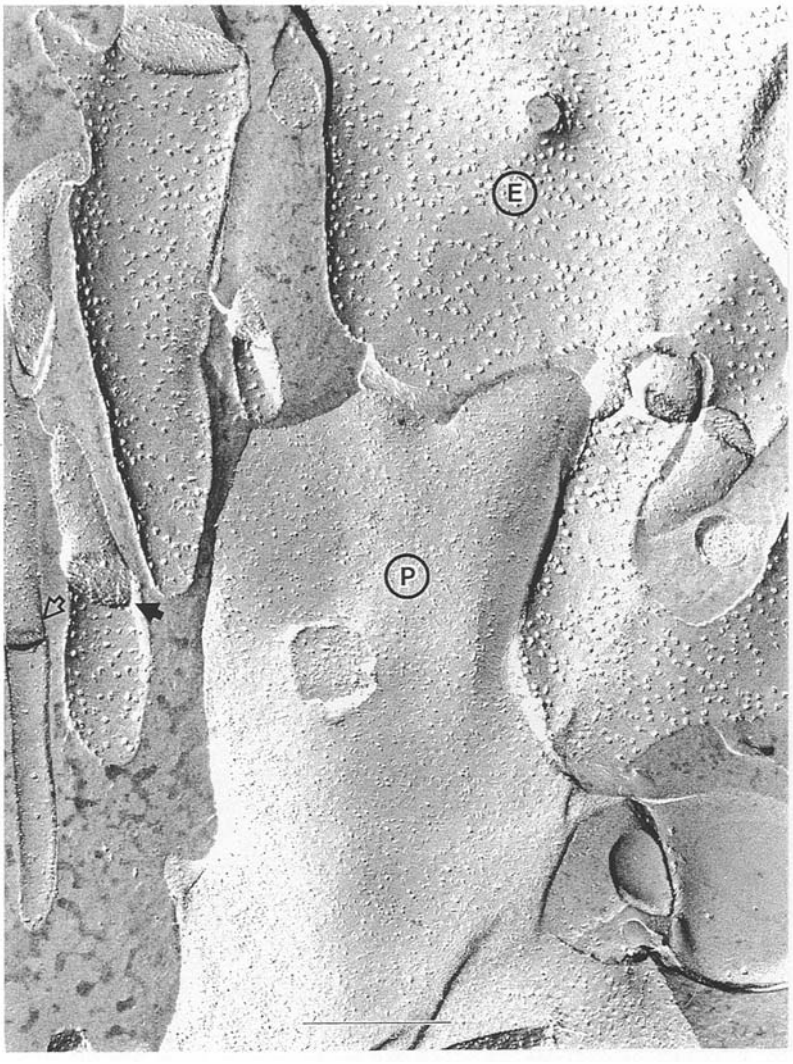

Fig. 5. The oolemma of water-injected oocytes have particles of different diameter and at different densities on the E and the P fracture faces. The E face has 14 nm diameter particles at a density of 886 ± 36 particles/μm^2. The P face, on the other hand, has particles of ~7 nm in diameter at a density of 212 ± 46 particles/μm^2 and large pits. Therefore, there are about four E face particles per each particle on the P face. The open arrow points to a microvillus fractured along the long axis. The black arrow points to a fold showing both the P and E fracture faces. Magnification: ×100,000, calibration bar: 0.3 μm.

CHIP AND MIP

Injection of cRNA coding for both CHIP and MIP increased the particle density on the P face of the oolemma only. CHIP appeared as a 9.3 ± 0.4 (mean, SD, n = 21) nm diameter intramembrane particle similar to those seen in proteoliposomes reconstituted with CHIP and in the P face of CHO cells transfected with this protein (Verbavatz et al., 1993, Zeidel et al., 1994). MIP appears as an 8.0 ± 0.6 (mean, SD n = 29) nm diameter intramembrane particle. Oocytes expressing large quantities of MIP (>4,000 particles/μm^2) contained particles aggregated into small patches exhibiting tetragonal symmetry similar to those in lens fiber cells (Zampighi et al., 1989) and in liposomes reconstituted with this protein (Dunia et al., 1987; Ehring et al., 1990).

The particle density of oocytes expressing MIP depended on the time of incubation postinjection and the concentration of cRNA injected. In oocytes from the same batch (i.e., dissected from one frog and injected at the same time), the density was 334 ± 77 (mean, SD, n = 7) particles/μm^2 at day one (Fig. 10*A*) and 1,085 ± 112 (mean ± SD, n = 6) particles/μm^2 at day two (Fig. 10*B*). The highest particle density was 4,109 ± 684 (mean, SD) particles/μm^2 which was measured in an oocyte three days postinjection (Fig. 10*C*).

In oocytes expressing CHIP and MIP, the particle density was correlated to the water permeability mea-

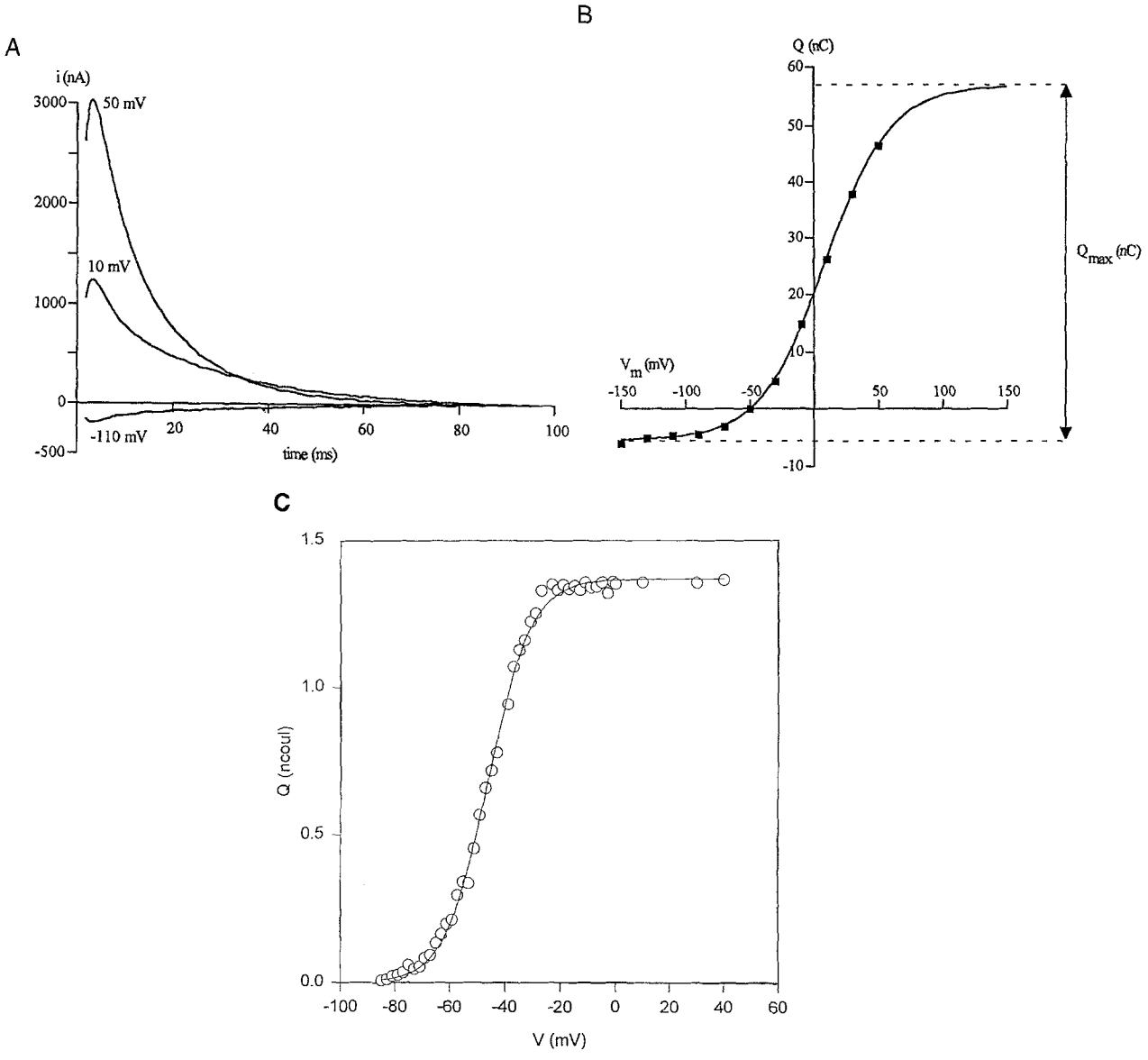

Fig. 6. Charge transfer (Q_{max}) of oocytes expressing SGLT1 was measured using the 2-electrode voltage clamp method (*Loo et al., 1993*). The oocytes were incubated in 100 mM NaCl buffer without sugar (*see* Materials and Methods) and the membrane potential clamped at −50 mV. The membrane potential was stepped to voltages ranging from −150 to +50 mV in 20 mV increments and the membrane currents recorded. Panel *A* shows compensated currents recorded for three voltage steps. At each voltage step, the charge movement Q was obtained from the integral of the transient current. Panel *B* shows a plot of *Q* against *V*(black squares) and the Boltzmann relation (continuous line) used to calculate the parameters Q_{max}, *z* and $V_{0.5}$. For the mutant *Shaker* K^+ channels, charge transfer was recorded by the cut-open oocyte technique (*Stefani et al., 1994*). The membrane potential was clamped at −90 mV and the transient currents obtained after stepping the potential to voltages ranging from −90 to +50 mV using the P/−4 procedure with a subtracting holding potential of −120 mV. The transient currents at each voltage were integrated to obtain the charge *Q*. Panel *C* shows a plot of *Q* were against *V* fitted by a Boltzmann relation with Q_{max} 1.4 nC, $z = 3.3$ and $V_{0.5} + -46$ mV.

sured in whole oocytes (Fig. 11). Neither CHIP nor MIP increased the membrane conductance or the charge transfer in oocytes (data not shown). Oocytes injected with cRNA coding for CHIP exhibited water permeabilities (P_f) that were ~35-fold larger than controls. Oocytes injected with cRNA coding for MIP, on the other hand, exhibited P_fs that were only ~12-fold greater than control oocytes (Fig. 11). Oocytes expressing SGLT1 (a sugar transporter) increased the water permeability by ~3-fold above controls.

P_f and the density of intramembrane particles were measured in oocytes obtained from the same batch. Oocytes expressing CHIP exhibited densities of 450 ± 83 (mean ± SD, n = 8, mean area counted = 0.63 μm^2)

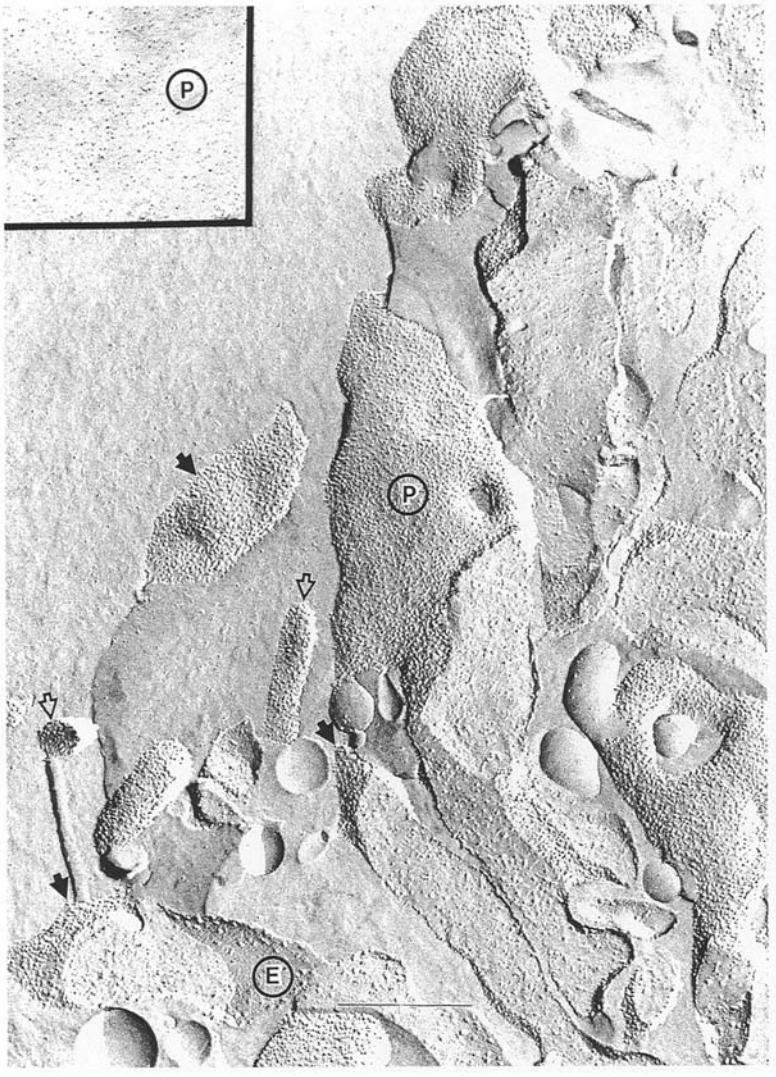

Fig. 7. The P fracture face of the oolemma of an oocyte expressing the Na/glucose cotransporter (SGLT1) at high density (Q_{max} > 30 nC). The density of 7 nm diameter particles on the P fracture face of the oolemma increased >4,000 μm^2. The oolemma, the folds and the microvilli exhibited similar particle densities which indicates that this protein is distributed homogeneously on the surface of the oocyte. The inset shows a P face of a control, water-injected oocyte, for comparison. Magnification: ×100,000, calibration bar: 0.3 μm.

particles/μm^2 while oocytes expressing MIP exhibited 4,109 ± 684 (mean ± SD, n = 7, mean area counted = 0.12 μm^2) particles/μm^2. From the ratio of P_f to particle density, the functional permeability per particle (p_f) was estimated to be 5.6×10^{-14} cm^3/sec for CHIP and 5.8×10^{-16} cm^3/sec for MIP. (These somewhat peculiar units can be understood if one realizes that this is the number of moles of water which would move through a single channel in one second under an osmotic gradient of one osmole per cm^3 or 1,000 osmolar.)

The estimate of p_f for MIP and its comparison to those of CHIP, a *bona fide* water transporter (Preston et al., 1992), and SGLT1 a sugar transporter, is indication that MIP is a water transporter in cells (*see also* Mulders et al., 1995). Comparison of the p_f estimated for all three molecules indicate that MIP exhibits a larger water permeability than controls and oocytes expressing SGLT1. However, MIP is ~100-fold less efficient than CHIP in conducting water (Fig. 11 and Table 2), a property that may prove important in understanding the function of this protein in lens fiber cells.

Discussion

Accurate estimates of the total number of cloned channels and transporters are required to express functional measurements made in whole oocytes as single-molecule capacities. Only in this manner can the efficiency of different clones and genetically engineered mutations can be compared di-

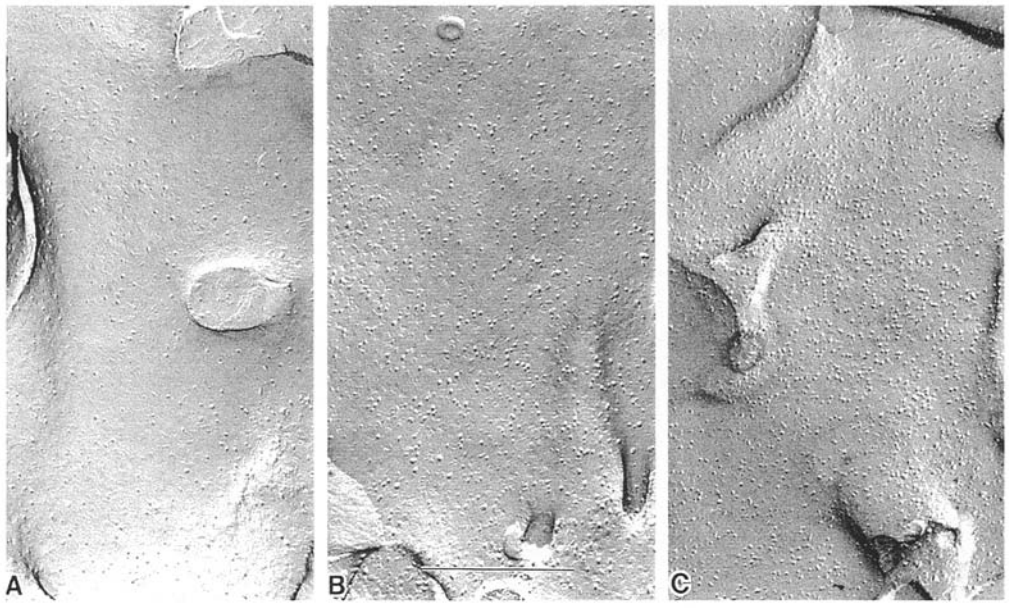

Fig. 8. The density of intramembrane particles on the P face of the oolemma of oocytes expressing SGLT1 was proportional to Q_{max}. Panels *A-C* show the *P* face of the oolemma of oocytes from where particle density (210 ± 55, particles/μm^2, 556 ± 108 particles/μm^2 and 655 ± 67 particles/μm^2), Q_{max} (4 nC, 11 nC and 16 nC) and total membrane capacitance (335 nF, 366 nF and 488 nF) were recorded. The values for particle density are after subtracting the density of particles present on the P face of water-injected, control oocytes. Magnification: *A-C:* ×100,000.

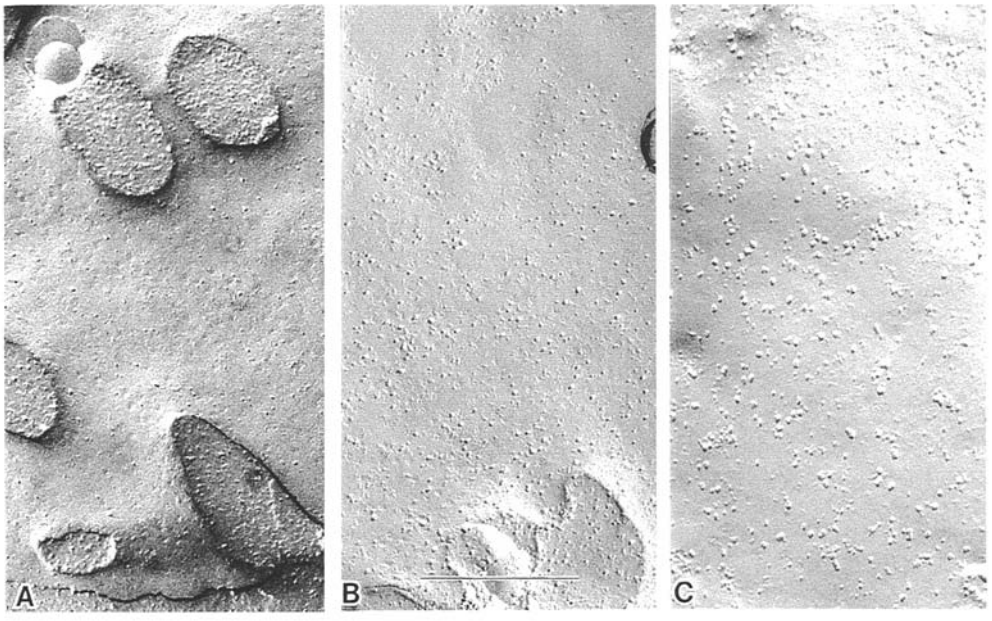

Fig. 9. The density of intramembrane particles on the P face of the oolemma in oocytes expressing the mutant *Shaker* K^+ channels was proportional to Q_{max}. Panels *A-C* show the P face of the oolemma from where particle density (~30 particles/μm, 368 ± 105 particles/μm^2, and 698 ± 110 particles/μm^2), charge transfer (0.2 nC, 1.66 nC and 3.2 nC) and total membrane capacitance (28.4 nF and 31.8 nF) were recorded. We have estimated gating charges of about 9 electronic charges per particle in these patches (Table 1). Magnifications: *A-C* 100,000, calibration bar: 0.3 μm.

rectly and evaluated. Traditionally, the number of channels has been estimated by electrophysiological or ligand-binding methods. The number of ion channels, such as K^+ or Na^+ channels, can be estimated from total conductance (G) and the conductance of the single channel (γ). The number of K^+ channels, N_k, for example, is calculated from the equation: $G_k = N_k \gamma P_o$, where G_k is the conductance to K^+ and P_o the probability of the open channel. This method

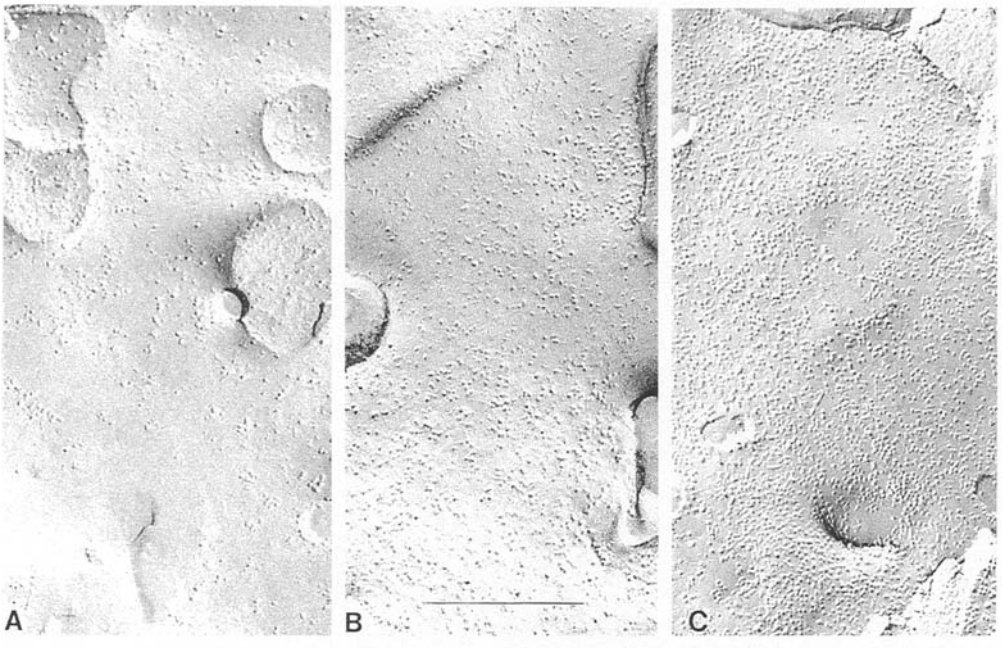

Fig. 10. The density of particles on the P face of the oolemma is proportional to the expression of the water transporter MIP. Panel *A* shows the P face of an oocyte that was injected with cRNA coding for MIP and incubated for 1 day in medium (334 ± 77 particles/μm^2). Panel *B* shows the P face of another oocyte from the same batch that was incubated for two days after injection (1085 ± 112 particles/μm^2). Panel *C* shows the particle density of an oocyte from a different batch that expressed the highest particle density (4,109 ± 684 particles/μm^2) which occurred three days post-injection. Magnification: ×100,000, calibration bar: 0.3 μm.

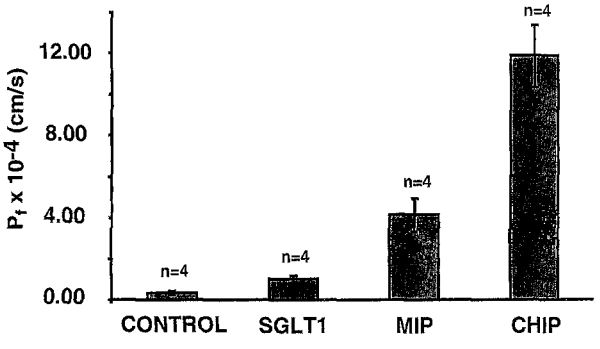

Fig. 11. Permeability to water (P_f) of whole-oocytes measured at 10°C. Bars represent mean of four oocytes with error bars ± SD. Control oocytes were injected with water, while oocytes expressing CHIP, MIP and SGLT1 were injected with ~4 ng, ~150 ng and 50 ng of cRNA respectively. All oocytes used to generate these data were prepared at UCLA.

has been used to estimate the number of conducting *Shaker* K^+ channels in the same patch where the gating charge was measured (Schoppa et al., 1992).

The number of channels or transporters can also be estimated from the density of charges transferred across the membrane field during voltage pulses. The *Q/V* data are fitted to a Boltzmann equation from which Q_{max} and *z*, the "effective valence" are calculated (Fig. 6). The number of channels and transporters, *N*, is calculated from the ratio Q_{max}/ze, where *e* is the charge of the electron. However, the number of channels or transporters estimated with this method is equal to the real number only when all the charge movement occurs in a single step (i.e., a two-state channel). Often channels are composed of several, nonidentical subunits. This molecular architecture greatly complicates the interpretation of the physical significance of the "effective valence." For example, the "effective valence" estimated from the Boltzmann fit of a channel or a transporter assembled from four identical, noninteracting subunits, each undergoing a single transition, will be exactly ¼ of the total gating charge (Bezanilla & Stefani, 1994) and *N*, calculated from the ratio Q_{max}/ze, will be overestimated by a factor of 4.

The number of channels or transporters can also be estimated by binding of specific, high affinity ligands. Charybdotoxin binds to some K^+ channels and phlorizin to SGLT1 with high affinity (Anderson et al., 1988; Toggenburger et al., 1978). Although charybdotoxin has been used to estimate the average number of K^+ channels in lymphocytes (Deutsch et al., 1991), no estimate of channel number using binding data on single oocytes has been published. The principal drawback of this method is, however, that many channels and transporters lack specific, high affinity ligands that can be used to estimate their number.

This paper validates a simple and accurate method of estimating the number of exogenously expressed intrinsic membrane proteins in oocytes. The method is

Table 2. Water Permeabilities of SGLT1, MIP and CHIP

Oocyte	$d(V/V_o)/dt$ s^{-1}	P_f (cm/s)	Particle density $(cm^2)^c$	p_f (Permeability per particle) $(cm^3/s)^e$	p_f (Permeability per monomer) $(cm^3/s)^d$
Water[b]	1.3×10^{-4}	1.1×10^{-4}	NA	NA	NA
SGLT1[a]	1.0×10^{-4}	1.0×10^{-4}	1.5×10^{11}	4.5×10^{-16}	NA
MIP[b]	3.8×10^{-4}	3.5×10^{-4}	4.1×10^{11}	5.8×10^{-16}	1.5×10^{-16}
CHIP[b]	2.9×10^{-3}	2.6×10^{-3}	4.5×10^{10}	5.6×10^{-14}	1.4×10^{-14}

[a] Oocytes were prepared at UCLA. Water permeability was the average of four oocytes. Particle density was measured on one oocyte (SGLT1-A1). Measurements were performed at 10°C and the challenge solution was Barth's plus genotomyocin diluted 70%. Control water permeability at 10°C was subtracted from SGLT1 permeability to calculate the permeability per particle.

[b] Oocytes were prepared at UCI. Permeability measurements were the average of 2–3 oocytes. Particle density estimates obtained from different oocytes from the same batch. Measurements were done at room temperature (~22°C) and the challenge solution was ND96 medium diluted 70%.

[c] Particle density measured above background.

[d] Assuming each MIP and Chip particle is a tetramer.

[e] Control water permeability was first subtracted before calculating permeability per particle.

based on the observations that water-injected control oocytes have an extremely low density of endogenous intramembrane particles (~200 particles/μm^2 instead of ~10,000 the loop of Henle (Verbavatz et al., 1993)) and that exogenously expressed channels and transporters appear as particles on the P face only. These properties allow the quantification of the density of intrinsic membrane proteins in the range of 100–5,000 particles/μm^2.

The accuracy of the number of channels and transporters estimated from the particle density depends exclusively in resolving the problem presented by the sampling of the large surface area of the oolemma. In this paper, the problem was solved by devising a method that produced extensive areas of P fracture face from different regions of the oocyte (vegetative and animal poles) and from folds and microvilli. We validated this method by showing that the ratio of Q_{max} to particle density remained constant in oocytes expressing very different amounts of either SGLT1 or *Shaker* K^+ channels (Table 1). Therefore, the density of intramembrane particles is a direct representation of the number of channels and transporters in the oolemma.

For SGLT1 and the mutant *Shaker* K^+ channels, the ratio of Q_{max} and the intramembrane particle density measured on the same oocyte allowed the calculation of "gating charges" of ~3.5 and of ~9 electronic charges per particle, respectively. The "gating charge" corresponds to the number of electrical dipoles or charges able to sense the potential drop across the membrane times the fraction of the electric field through which they move. The larger "gating charge" estimated in the mutant *Shaker* K^+ channels suggests that this protein undergoes a larger number of voltage-dependent states than the cotransporter.

The "gating charge" estimated from the ratio of Q_{max} to the density of particles was compared to the "effective valence" (z) calculated by fitting a Boltzmann equation to the same Q/V data (Fig. 6). For both SGLT1 and the mutant *Shaker* K^+ channels, the gating charge was ~3-fold higher than the "effective valence" calculated from the fit. Such a discrepancy is not unexpected because the "effective valence" is equivalent to the "gating charge" of a channel or transporter only if all the charge movement occurs in a single step (Bezanilla & Stefani, 1994).

For the conducting *Shaker* K^+ channels, Shoppa et al. (1992) estimated 12 electronic charges per channel using the conductance method described previously. Our method estimated 9 electronic charges per particle. The small difference of both estimates, if significant, may be due to the fact that our method estimates the total number of channels and not just those that conduct ions when a voltage difference is applied to the membrane. An alternative explanation that cannot be ruled out is that the mean particle density is an overestimate of the number of channels because other intrinsic membrane proteins were inserted together with the newly synthesized channels.

The generality of the method is emphasized by estimating the number of channels in the plasma membrane of oocytes expressing the water transporters CHIP and MIP. These intrinsic membrane proteins do not induce ionic conductance or exhibit charge transfer and lack high affinity specific ligands. This study and the work of Mulders et al. (1995) provide definitive evidence that, in oocytes, MIP is a water transporter. Our conclusion is based on the comparison of the single particle water permeability of MIP with those estimated for CHIP, a well-established water transporter, SGLT1, a sugar transporter and control oocytes. For CHIP, we estimated a single-molecule permeability, p_f of 1.4×10^{-14} cm^3/sec that is ⅓ of that calculated in proteoliposomes reconstituted with the purified protein ($\sim 4 \times 10^{-14}$ cm^3/sec; Zeidel et al., 1994). Our value agrees well with that of 1×10^{-14} cm^3/sec reported for CHIP expressed in oocytes by Preston et al. (1992). The single particle water permeability of MIP was estimated to be 1.5×10^{-16} cm^3/sec. This number is substantially smaller than the per-

meability for CHIP. Thus, our studies indicate that, in oocytes, MIP is a water transporter about 100-fold less effective than CHIP in transporting water through the oolemma. The question that remained to be answered, however, is the significance of water permeability in the lens, an organ that expressed large amounts of MIP.

In conclusion, freeze-fracture methods can be applied to estimate the number of exogenously expressed proteins in the plasma membrane of *Xenopus* oocytes. The method is simple, general and accurate and, in principle, can be applied to all intrinsic membrane protein exogenously expressed in oocytes. The fact that function and particle density can be measured *on the same oocyte* facilitates measurements of the functional properties of single molecules of channels, transporters and receptors.

We thank Manoli Contreras for preparation and injection of oocytes. This work was supported by NIH Grants EY-04110 (to GAZ), DK-19567 (to EW), GM30376 (to F.B.) and EY-05661 (to J.E.H.).

References

Anderson, C.S., MacKinnon, R., Smith, C., Miller, C. 1988. Charybdotoxin block of single Ca^{2+} activated K^+ channels. Effect of channel gating, voltage, and ionic strength. *J. Gen. Physiol.* **91:**317–ui333

Barnard, E.A., Miledi, R., Sumikawa, K. 1982. Translation of exogeneous messenger RNA encoding for nicotinic acetylcholine receptors produces functional receptors in *Xenopus* oocytes. *Proc. R. Soc. Lond. Ser. B.* **215:**241–246

Bezanilla, F., Armstrong, C.M. 1977. Inactivation of the sodium channel I. Sodium current experiments. *J. Gen. Physiol.* **70:**549–566

Bezanilla, F., Perozo, E., Stefani, E. 1994. Gating of *Shaker* K channels. II. The components of gating currents and a model of channel activation. *Biophys. J.* **66:**1011–1021

Bezanilla, F., Stefani, E. 1994. Voltage-dependent gating of ionic channels. *Ann. Rev. Biomol. Struct.* **23:**819–846

Bluemink, J.G., Hage, W.J., van den Hoef, M.H.F., Dictus, W.J.A.G. 1983. Freeze-fracture electron microscopy of membrane changes in progesterone-induced oocytes and eggs of *Xenopus laevis*. *Eur. J. Cell Biol.* **31:**85–93

Deutsch, C., Price, M., Lee, S., King, V.F., Garcia, M.L. 1991. Characterization of high binding sites for charybdotoxin in human T lymphocytes. Evidence for association with the voltage-gated K^+ channel. *J. Biol. Chem.* **266:**3668–3674

Dick, E.G., Dick, D.A.T. 1970. The effect of microvilli on the water permeability of single toad oocytes. *J. Cell Sci.* **6:**451–476

Dunia, I., Manenti, S., Rousselet A., Benedetti, E.L. 1987. Electron microscopic observations of reconstituted proteoliposomes with the purified major intrinsic protein of the eye lens fibers. *J. Cell Biol.* **105:**1679–1689

Ehring, G.R., Zampighi, G.A., Horwitz, J., Bok, D., Hall, J.E. 1990. Properties of channels reconstituted from major intrinsic protein of lens fiber membranes. *J. Gen. Physiol.* **96:**631–664

Gorin, M.B., Yancey, S.B., Cline, J., Revel, J.P., Horwitz, J. 1984. The major intrinsic protein of lens fiber membrane: Characterization and structure based on cDNA cloning. *Cell* **39:**49–56

Li, M., Unwin, N., Stauffer, K.A., Jan, Y-N, Jan, L.Y. 1994. Images of purified *Shaker* potassium channels. *Curr. Biol.* **4:**110–115

Loo, D.D.F., Hazama, A., Supplisson, S., Turk, E., Wright E.M. 1993. Relaxation kinetics of the Na^+ glucose cotransporter. *Proc Natl. Acad. Sci. USA* **90:** 5767–5771

MacKinnon, R. 1991. Determination of the subunit stoichiometry of a voltage-activated potassium channel. *Nature* **350:**232–235

Mulders, M.S., Preston, G.M., Deen, M.T., Guggino, W.B., van Os, C.H., Agre, P. Water channel properties of Major Intrinsic Protein (MIP) of lens. *J. Biol. Chem.* (*in press*)

Parent, L., Supplisson, S., Loo, D.F., Wright, E.M. 1992. Electrogenic properties of the cloned Na^+/glucose cotransporter. I. Voltage-clamp studies. *J. Membrane Biol.* **125:**49–62

Perozo, E., MacKinnon, R, Bezanilla, F., Stefani, E. 1993. Gating currents from a nonconducting mutant reveal open-closed conformations in *Shaker* K^+ channels. *Neuron* **11:**353–358

Preston, G.M., Agre, P. 1991. Isolation of the cRNA for erythrocyte integral membrane protein of 28 KD member of an ancient channel family. *Proc. Natl. Acad. Sci. USA* **88:**11110–11114

Preston, G.M., Jung, J.S., Guggino, W.B., Agre, P. 1992. Appearance of water channels in *Xenopus* oocytes expressing red cell CHIP28 protein. *Science* **256:**385–387

Schoppa, N.E., McCormack, K., Tanouye, M.A., Sigworth, F.J. 1992. The size of gating charge in wild-type and mutant *Shaker* potassium channels. *Science* **255:**1712–1715

Stefani, E., Toro, L., Perozo, E., Bezanilla, F. 1994. Gating of *Shaker* K^+ channels: I. Ionic and gating currents. *Biophys. J.* **66:**996–1010

Taglialatela, M., Toro, L., Stefani, E. 1992. Novel voltage clamp to record small, fast currents from ion channels expressed in *Xenopus* oocytes. *Biophys. J.* **61:**78–82

Toggenburger, G., Kessler, M., Rothstein, A., Semenza, G., Tannenbaum, C. 1978. Similarity in effects of Na gradients and membrane potentials on D-glucose transport by, and phlorizin binding to, vesicles derived from brush border of rabbit intestinal mucosal cells. *J. Membrane Biol.* **40:**269–290

Verbavatz, J.M., Brown, D., Sabolic, I., Valenti, G., Ausiello, D.A., Vanhoek, A.N., Ma, T., Verkman, A.S. 1993. Tetrameric assembly of CHIP28 water channels in liposomes and cell membranes. A freeze-fracture study. *J. Cell Biol.* **123:**605–618

Zampighi, G.A., Kreman, M., Ramon, F., Moreno, A.L., Simon, S.A. 1988. Structural characteristics of gap junctions. I. Channel number in coupled and uncoupled conditions. *J. Cell Biol.* **106:**1667–1678

Zampighi, G.A., Hall, J.E., Ehring, G.R., Simon, S.A. 1989. The structural organization and protein composition of lens fiber junctions. *J. Cell Biol.* **108:**2255–2275

Zeidel, M.L., Nielsen, S., Smith, B.L., Ambudkar, S.V., Maunsbach, A.B., Agre, P. 1994. Ultrastructure, pharmacological inhibition and transport selectivity of aquaporin channel-forming integral protein in proteoliposomes. *Biochemistry* **33:**1606–1615

Zhang, R., Verkman, A.S. 1991. Water and urea permeability properties of Xenopus oocytes: expression of mRNA from toad urinary bladder. *American J. Physiol.* **260**(Cell Physiol. 29) C26-C34